

Original Article

EXPERIMENTAL STUDY ON THE MAIN INFLUENCING FACTORS OF INDUCED MEMBRANE-GUIDED SPONTANEOUS OSTEOGENESIS

J. Liu^{1,§}, Q.D. Yin^{1,§}, F.Y. Bu^{1,*} and X.M. Chen^{1,*}¹Department of Orthopaedics, Wuxi Ninth People's Hospital Affiliated to Soochow University, 214063 Wuxi, Jiangsu, China

§These authors contributed equally.

Abstract

Background: Induced membrane-guided spontaneous osteogenesis (IMGSO) has been experimentally validated, but there is a lack of research on its cause and influencing factors. The aim of this study was to investigate the main influencing factors of IMGSO. **Methods:** Seventy-two adult Sprague-Dawley rats with 10- or 15-mm femur defects were established and randomly divided into 6 groups (n = 12). Except for the control group (Group B4), all the defects were filled with vancomycin-loaded polymethyl methacrylate bone cement spacers. Size-matched spacers for Groups A1–A2 and B1, larger spacers for Group B2, and bone ends sealed for Group B3. The osteogenic activities of different parts of the induced membrane (IM) in Groups A1–A2 and spontaneous osteogenic manifestations in Groups B1–B4 were observed. **Results:** At 5 weeks, the number of bone mesenchymal stem cells and the protein and mRNA expression levels of bone morphogenetic protein-2 (BMP-2), transforming growth factor- β 1 (TGF- β 1) and vascular endothelial growth factor (VEGF) in the proximal and distal parts of the IMs were similar and greater than those in the middle part ($p < 0.05$). At 12 weeks, Group B1 had more new bone formation along the IM originated from the bone end than Group B2 ($p < 0.05$), while Groups B3 and B4 had no new bone, only bone resorption and bone atrophy. **Conclusions:** The osteogenic activities of different parts of the IMs vary, with the strongest activity in the IM near the bone end. Bone marrow overflowing of the bone end enhances the osteogenic activities of the IMs, resulting in IMGSO, and is the key factor. Another main influencing factor of IMGSO is the maintenance of an appropriate membrane size.

Keywords: Bone defect, induced membrane, membrane-guided bone regeneration, bone cement, new bone formation.

***Address for correspondence:** F.Y. Bu, Department of Orthopaedics, Wuxi Ninth People's Hospital Affiliated to Soochow University, 214063 Wuxi, Jiangsu, China. Email: bofanyuyqd@163.com; X.M. Chen, Department of Orthopaedics, Wuxi Ninth People's Hospital Affiliated to Soochow University, 214063 Wuxi, Jiangsu, China. Email: mingyin031@163.com.

Copyright policy: © 2025 The Author(s). Published by Forum Multimedia Publishing, LLC. This article is distributed in accordance with Creative Commons Attribution Licence (<http://creativecommons.org/licenses/by/4.0/>).

Introduction

Nyman *et al.* [1] reported in their study of periodontal tissue regeneration, that a membrane placed between the periodontal connective tissue flap and the tooth root as a barrier could prevent the epithelium and connective tissue at the gum bonding level from growing into the periodontal tissue, selectively guiding regenerative potential cells to proliferate toward the surface of the tooth root and producing new cementum and periodontal ligament. Therefore, they proposed membrane-guided tissue regeneration (MGTR). Inspired by MGTR, Buser *et al.* [2] proposed membrane-guided bone regeneration (MGBR), which refers to the use of barrier membranes to exclude nonosteoblastic cells from invading the defect while creating a bone growth space that allows osteoblasts to preferentially migrate and grow. Membranes made of various ma-

terials have been proven to serve as MGBR, which usually requires a bone graft within the membrane to repair bone defects [3–5]. However, animal experiments have shown that without bone graft within the membrane, a small amount of new bone can be formed, and even the new bone can complete bone defect repair in MGBR [1,6]. However, they did not describe the characteristics and influencing factors for the new bone. In standard MGBR, bone grafting is necessary.

The Masquelet induced membrane technique (IMT) is a two-stage surgical procedure used to reconstruct segmental bone defects. During the first surgery, diseased or injured tissue is removed, and the bone defect is filled with a polymethyl methacrylate (PMMA) cement spacer [7–11]. During the second surgery, the spacer is removed through a longitudinal incision and the autograft is filled within the

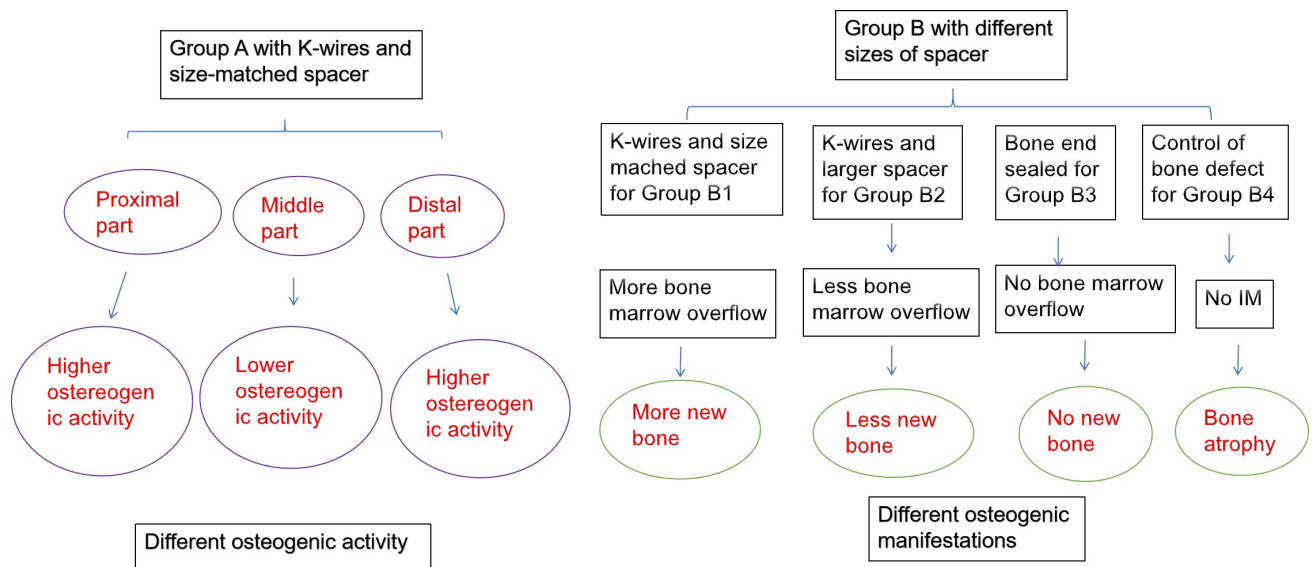


Fig. 1. The schematic diagram of methodology and results. IM, induced membrane.

induced membrane (IM). The IMT is also a type of MGBR, and the IM is not a ready-made membrane but a biomembrane that slowly forms in the body. Both Klaue *et al.* [12] and Gruber *et al.* [13] noted that a small amount of new bone formed in the IM near the bone end after 2–3 months of filling with PMMA in animal femoral defects. However, they also did not describe the characteristics and influencing factors for the new bone.

The callus formed after cancellous bone grafting is usually called new bone. To distinguish the calluses formed by bone grafts from those formed by nonbone grafts, we named the former without bone graft material within the IM as spontaneous osteogenesis (SO). We reported the use of IM-guided SO (IMGSO) in rats and a few cases [14–16]. It was speculated that bone marrow overflowing from the bone end enhances the osteogenic activity of the IM, potentially leading to SO. However, this speculation has not been experimentally verified. Standard IMT requires two-stage surgery. In addition, for large bone defects, a significant amount of autogenous bone graft material is needed, but the amount of autogenous bone material obtained is limited. Therefore, two-stage surgery and the need for more autogenous bone material are the main drawbacks of the IMT [17]. One-stage surgery with minimal or no autogenous bone graft material has become a research direction for IMT [15,18,19]. Nevertheless, the IMGSO phenomenon makes it possible for surgeons to perform one-stage surgery or bone marrow graft instead of autogenous bone graft material using an improved IMT to reconstruct bone defects [16]. Therefore, IMGSO is a promising research direction.

It is necessary to understand the cause and influencing factors of IMGSO prior to repairing bone defects with IMGSO. However, there is a lack of research on the cause and influencing factors of IMGSO. Therefore, the aim of this study is to investigate the main influencing factors of

IMGSO. Because newly formed bone always grows along the IM from the bone end to the defect center, we hypothesized that the proximal or distal part of the IM has stronger osteogenic activity than the middle part does and that the formation of new bone is influenced by the amount of bone marrow and the appropriate size of the membrane at the bone end.

Materials and Methods

Grouping and Housing Conditions

Seventy-two specific pathogen-free adult male Sprague-Dawley rats purchased from Suzhou Baisheng Biotechnology Co., Ltd. (Suzhou, China; mean weight, 281 g; range, 230–305 g) were randomly divided into 6 groups ($n = 12$). Groups A1–A2 were used to observe the osteogenic activity of different parts (proximal, middle, and distal) of the IMs formed at 5 weeks so that a 15-mm osteotomy was needed (otherwise, there would be too few membranes in each part), whereas Groups B1–B4 were used to observe the osteogenic manifestations of the IMs formed at 12 weeks so that only a 10-mm osteotomy was needed. According to the preliminary experiment, the average diameter of the shaft of the rat femur was 4 mm. Two sizes of spacers with a diameter of 4 mm for the size-matched group and 6 mm for the larger size were prepared with vancomycin-loaded PMMA (2 g/40 g) (CMW 3, DePuy International, Blackpool, UK) and hardened in silicone molds (6035H, Blank Flame Medical, Shanghai, China). The methodology is summarized in Fig. 1. The spacer samples were sterilized with ethylene oxide. The animals were allowed to acclimate for 1 week at the animal experiment center (Soochow University Laboratory Animal Research Center, Suzhou, China; temperature: 20–23 °C; day/night light cycle: 12/12 (h/h);

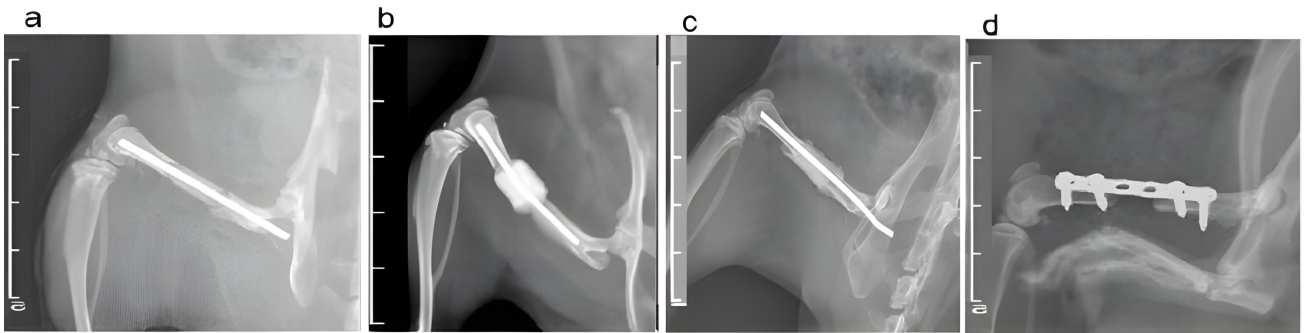


Fig. 2. Bone defect model. (a) A size-matched spacer was used to fill the defect. (b) A larger spacer was fabricated to fill the defect. (c) Bone cement connects the spacer and bone end to seal the bone end. (d) Blank control.

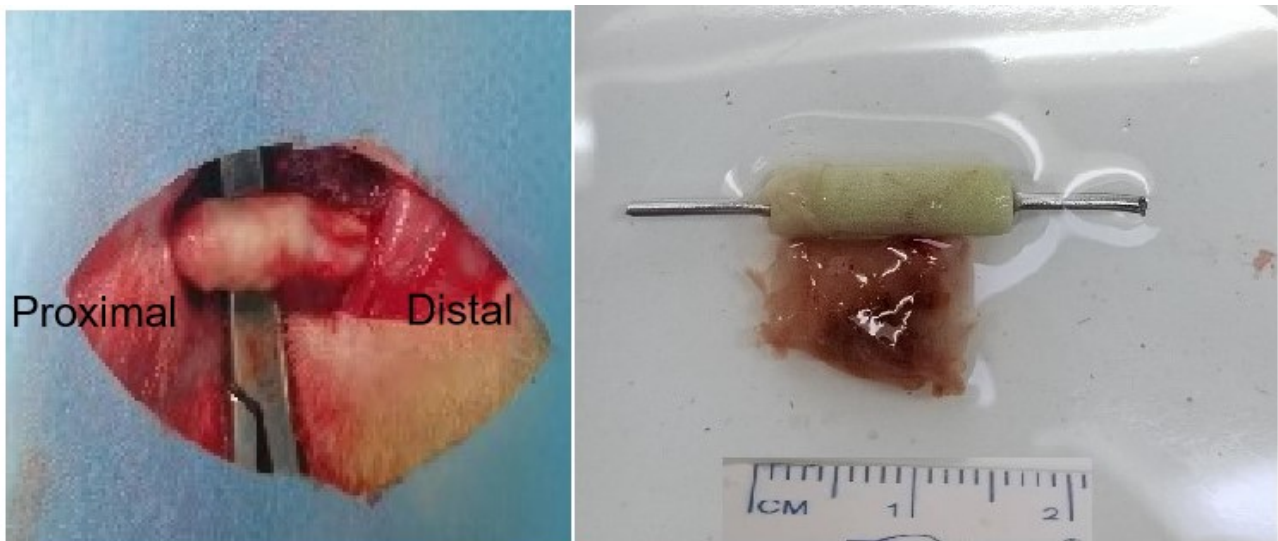


Fig. 3. The induced membrane.

humidity: 60 %–80 %; freely available sterile complete feed (Anlimo, Nanjing, China) and filtered water) prior to the experiments.

Surgical Procedure

Five percent pentobarbital (45 mg/kg) was injected intraperitoneally to induce general anesthesia. The surgical area was shaved and then disinfected with iodophor. A 3-cm incision was made in the skin and muscles on the dorsal side parallel to the long axis of the right femoral bone, and the subcutaneous muscles were separated to expose the shaft of the femur. Two osteotomies were created using a swing saw to remove a 15-mm midshaft bone fragment (including the periosteum) from Group A and a 10-mm midshaft bone fragment (including the periosteum) from Group B. In Groups A1–A2 and B1, size-matched spacers of $4 \times 15 \text{ mm}^2$ or $4 \times 10 \text{ mm}^2$ were used to fill the defect (Fig. 2a). In Group B2, larger spacers of $6 \times 10 \text{ mm}^2$ were used to fill the defect (Fig. 2b). In Group B3, a small amount of bone cement was used to connect the size-matched spacer and bone end, sealing the bone marrow (Fig. 2c). The defects

in Groups A1–A2 and B1–B3 were intramedullary fixed with 1.4-mm Kirschner wires. Considering the instability of fixation using Kirschner wires alone, the bone defects in Group B4, the control group, were fixed with 1.5-mm plates (Fig. 2d). Finally, the muscles were repositioned and the incisions were closed with bioresorbable suturing material. The animals were monitored daily after surgery. Within 3 days of the operation, 4×10^4 U penicillin sodium was injected intramuscularly to prevent infection and the animals were raised in a single cage until the surgical incision healed. The surgery procedure was performed by the first and second authors.

Osteogenic Activity Analysis of the IMs in Different Areas

The rats in Groups A1–A2 were euthanized with an overdose (130 mg/kg) of pentobarbital administered intraperitoneally at 5 weeks after surgery, after which the animals were disinfected and spread on towels, and the original surgical site was reopened. The IMs around the spacer were harvested by separating the surrounding muscles and were equally divided into proximal, middle and distal parts (Fig.

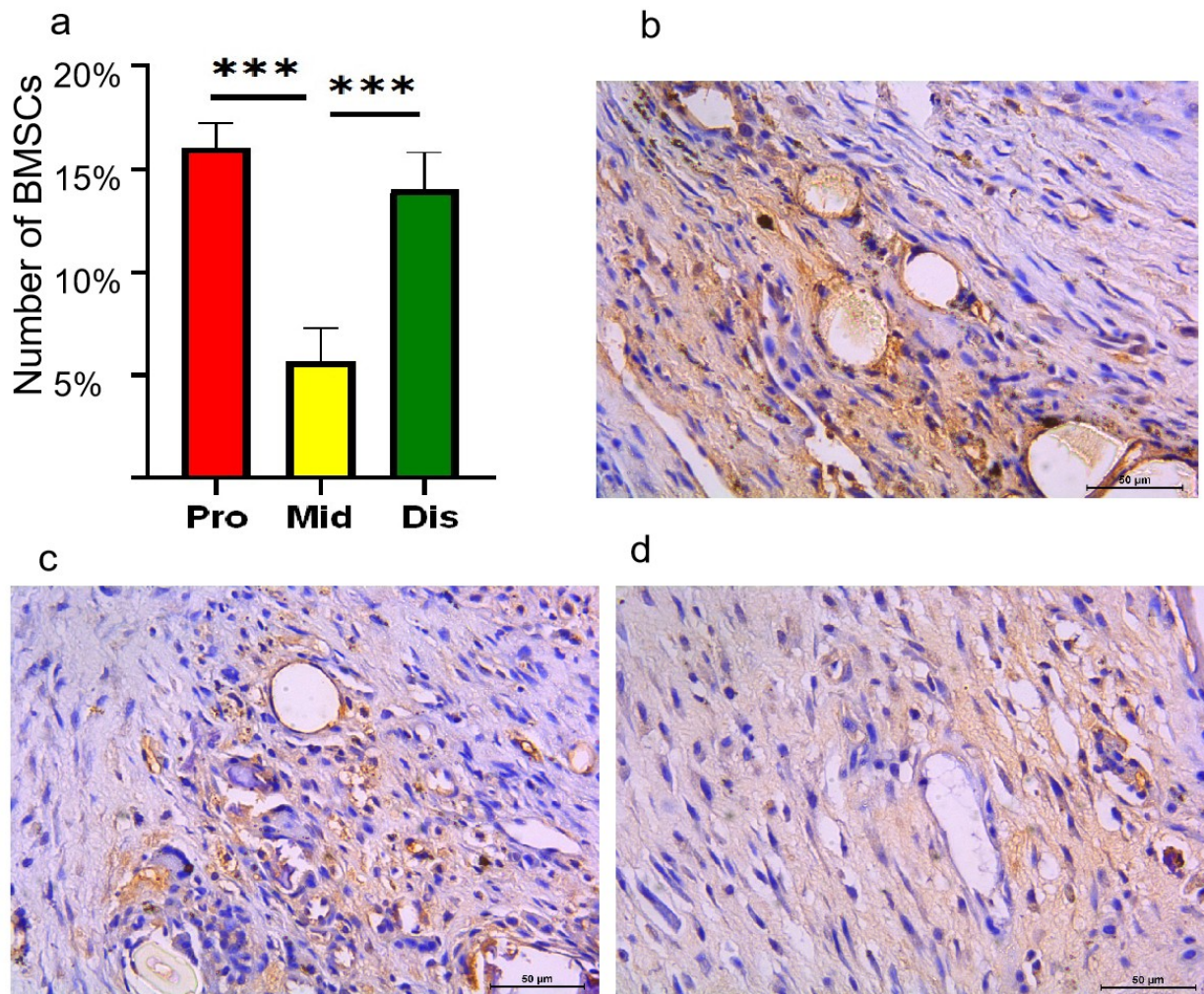


Fig. 4. BMSCs of the IMs in different areas at 5 weeks. (a) Column graph comparing the relative number of STRO-1-positive cells in different parts of the IMs. The numbers of BMSCs among the IMs in the (b) distal and (c) proximal parts were similar and greater than those in the middle part (d) ($n = 12$; mean \pm SD; $\times 400$; Brown indicates BMSCs; ns, no significant difference; $***p < 0.001$; BMSC, bone mesenchymal stem cell; IM, induced membrane; SD, standard deviation).

3). The IMs in Group A1 were fixed in 4% paraformaldehyde to observe the number of bone mesenchymal stem cells (BMSCs), and the IMs in Group A2 were put into cryopreservation tubes and immediately stored in liquid nitrogen to measure the protein and mRNA expression levels of related factors of the IMs in the proximal, middle and distal parts.

BMSC measurement (Wuxi Huaixin Biomedical Technology Co., Ltd.): The levels of BMSCs in the IMs in different areas were measured using an immunohistochemical quantitative method by detecting STRO-1-positive cells. The IM was placed in 10% formaldehyde for 24 h and removed to prepare 5 μm thick slices. After processing according to conventional procedures, anti-rat STRO-1 (1:200, MAB1038, R&D Systems, Wiesbaden, Hesse, Germany) was added dropwise and the mixture was incubated overnight at 4 $^{\circ}\text{C}$ in the dark. Horseradish peroxidase (HRP)-labeled sheep anti-mouse secondary antibody

(1:1000) was added dropwise and the mixture was incubated at 37 $^{\circ}\text{C}$ for 1 h. 3,3'-Diaminobenzidine (DAB) staining solution was added dropwise and the mixture was incubated at room temperature for 10 minutes. The mixture was incubated with hematoxylin staining solution at room temperature for 30 seconds. Dehydrated, transparent, and sealed cells were observed under a light microscope and the cells that were stained yellow brown were considered STRO-1-positive cells. Three fields of view were selected for each slice under a 400x microscope, optical density analysis was performed using Image J software (V1.8, NIH, Bethesda, MD, USA), the average percentage of positive cells was recorded, and IBM-SPSS Statistics 26.0 SPSS (Armonk, NY, USA) was used for statistical analysis.

Western blotting: The cryopreservation tube was removed and Western blotting was performed to measure the expression levels of bone morphogenic protein-2 (BMP-2), transforming growth factor- β 1 (TGF- β 1) and vascu-

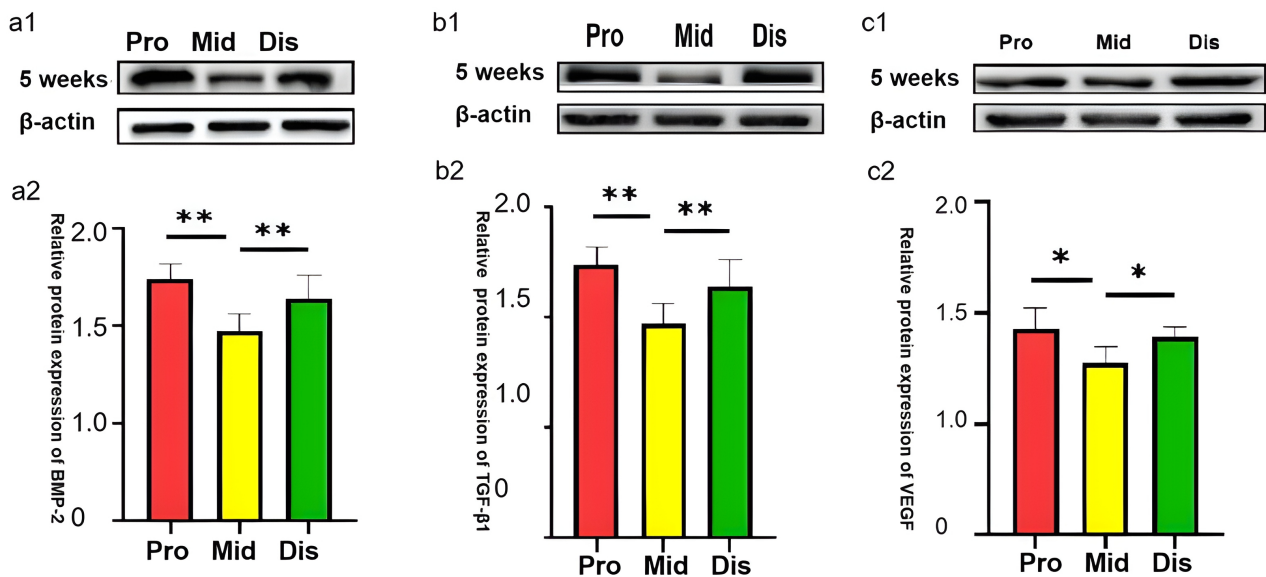


Fig. 5. Western blot analysis of BMP-2, TGF- β 1 and VEGF in different parts of the IMs at 5 weeks. (a1) Images and (a2) quantification of Western blot bands of BMP-2. (b1) Images and (b2) quantification of Western blot bands of TGF- β 1. (c1) Images and (c2) quantification of the Western blot bands of VEGF ($n = 12$; mean \pm SD; * $p < 0.05$; ** $p < 0.01$; BMP-2, bone morphogenic protein-2; TGF- β 1, transforming growth factor- β 1; VEGF, vascular endothelial growth factor).

lar endothelial growth factor (VEGF) protein in the IMs from different areas. Proteins were extracted from the IMs using radioimmunoprecipitation assay (RIPA) lysis buffer (P0013C; Beyotime Institute of Biotechnology, Nantong, China) and quantified using a bicinchoninic acid (BCA) protein assay kit (P0011; Beyotime Institute of Biotechnology, Shanghai, China). The extracted protein was subjected to sodium dodecyl sulfate-polyacrylamide gel electrophoresis (SDS-PAGE) and transferred to a polyvinylidene fluoride (PVDF) membrane. The PVDF membranes containing the target bands were incubated overnight with the corresponding primary antibodies at 4 °C. Next, the target bands were detected with a CFX96 Real-Time System (Bio-Rad, USA) after the corresponding secondary antibodies were incubated for 1 h. Quantification of the blots was performed using ImageJ software and the expression levels of the target proteins were normalized to those of β -actin. The following antibodies were used: anti-BMP-2 (ab214821; Abcam, Shanghai, China), anti-TGF- β 1 (ab215715; Abcam, Shanghai, China), and anti-VEGF (ab46154; Abcam, Shanghai, China).

Quantitative RT-PCR (qRT-PCR): The cryopreservation tube was removed, and qRT-PCR was used to measure the mRNA expression levels of BMP-2, TGF- β 1, and VEGF in the IMs from different areas. Total RNA was extracted using TRIzol Reagent (15596026CN; Thermo Fisher Scientific, Waltham, MA, USA) and reverse-transcribed into cDNA. qRT-PCR was performed using an UltraSYBR mixture (15596018; Jiangsu CoWin Biotech, Co., Ltd., Beijing, China). The expression of each gene was normalized to that of the housekeeping gene,

Table 1. Genes and sequences.

Gene name	Sequence
<i>Vegf</i>	Forward 5'-TCCTGTGTGCCCTAATGC-3' and Reverse 5'-ACGCACTCCAGGGCTTCAT-3'
<i>Bmp-2</i>	Forward 5'-CTTTTGCCACGACGGTAAA-3' and Reverse 5'-TGCCTTTTGCAGCTGGACTT-3'
<i>Tgf-β1</i>	Forward 5'-GACTCTCCACCTGCAAGACCAT-3' and Reverse 5'-GGACTGGCGAGCCTTAGTTT-3'
<i>Gapdh</i>	Forward 5'-GTATGACTCTACCCACGGCAAGT-3' and Reverse 5'-TCTCGCTCCTGGAAGATGGT-3'

glyceraldehyde-3-phosphate dehydrogenase (GAPDH), in a selected control sample. The main genes and sequences were listed in Table 1.

Osteogenic Manifestations

The rats in Groups B1–B4 were euthanized 12 weeks after surgery, the spacers, intramedullary Kirschner wires and plates were removed, and the femoral specimens were removed for radiographic, gross and histological examinations to observe new bone in the IMs.

The length of new bone formed was defined as the average of the longest distance of new bone growth from the proximal and distal bone ends to the center of the bone defect, as measured by X-ray or the naked eye.

Histological examination: Ossified tissue was fixed in 4 % paraformaldehyde for 48 h in sequence, soaked in

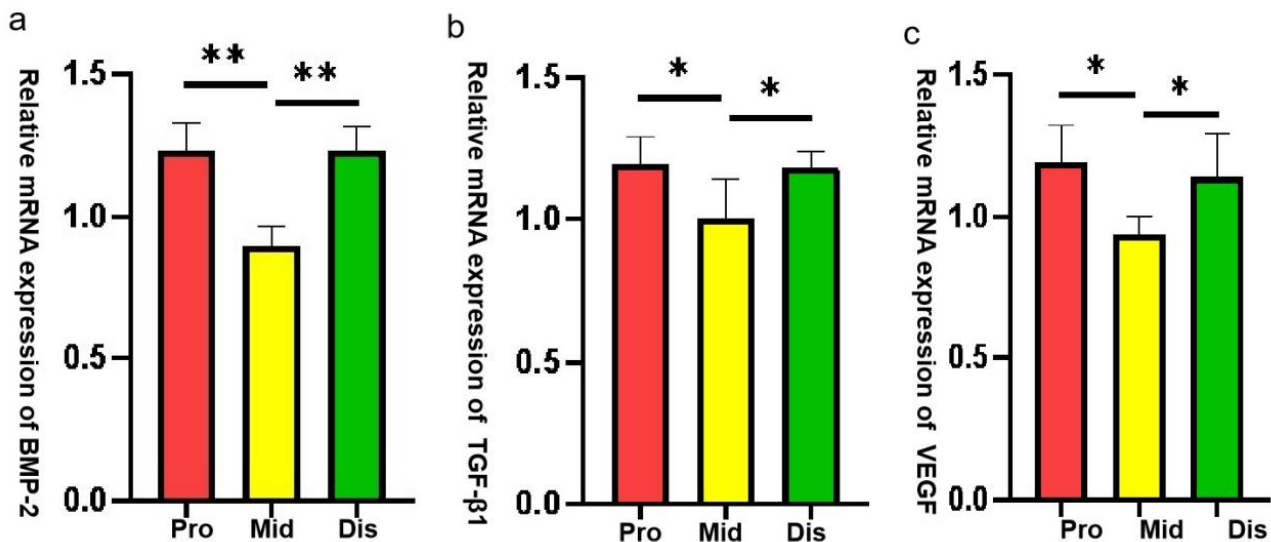


Fig. 6. Relative mRNA expression of factors. (a) BMP-2, (b) TGF- β 1 and (c) VEGF in different parts of the IMs at 5 weeks ($n = 12$; mean \pm SD; * $p < 0.05$; ** $p < 0.01$; BMP-2, bone morphogenic protein-2; TGF- β 1, transforming growth factor- β 1; VEGF, vascular endothelial growth factor).

decalcifying solution for 1 month, embedded in paraffin, sliced (4 μ m thickness), and stained with safranin O-fixed green. The tissue composition was observed under a light microscope.

Statistical Analysis

Statistical analysis was performed using SPSS software (version 21.0; IBM, Armonk, NY, USA). Multiple group comparisons were analyzed with one-way analysis of variance (ANOVA), and further pairwise comparisons were performed via the least significant difference (LSD) test. The values are reported as the mean \pm standard deviation (SD), with $p < 0.05$ considered statistically significant.

Results

Osteogenic Activity

BMSC Measurement

At 5 weeks, the numbers of BMSCs in the IMs from the 3 areas were significantly different ($F = 206.321$, $p < 0.001$) (Fig. 4a), and the numbers of BMSCs in the IMs from the distal and proximal areas (Fig. 4b,c) were similar (15.83 % \pm 1.95 % and 14.75 % \pm 0.97 %, respectively) and greater than those in the middle area (Fig. 4d) (5.38 % \pm 1.02 %) ($p < 0.001$).

Western Blotting

The gray values, including the images and quantification, of the protein bands revealed that the protein expression levels of BMP-2 (Fig. 5a1,a2), TGF- β 1 (Fig. 5b1,b2) and VEGF (Fig. 5c1,c2) in the IMs in the proximal and distal parts at 5 weeks were similar and significantly greater than those in the middle part ($p < 0.05$).

qRT-PCR

The qRT-PCR results revealed that the mRNA expression levels of BMP-2 (Fig. 6a), TGF- β 1 (Fig. 6b) and VEGF (Fig. 6c) in the IMs in the proximal and distal parts at 5 weeks were significantly greater than those in the middle part ($p < 0.05$).

Osteogenic Manifestations

X-ray (Fig. 7a) and gross (Fig. 7b) examinations of Group B1 revealed that the gap between the spacer and the bone end disappeared completely at 12 weeks and obvious new bone formed from the bone end and grew along the IM, with an average length of 3.4 ± 0.4 mm. The gap between the spacer and the bone end in Group B2 partially disappeared and only a small amount of new bone was observed. The length of new bone formed ranged between 0 and 2 mm, with an average of 0.5 ± 0.1 mm. The IMs in Group B3 neither thickened nor hardened, and bone atrophy was observed at the bone end. The bone ends of Group B4 were wrapped in soft tissue, leading to bone resorption or atrophy. New bone formed significantly differently among the four groups ($F = 27.437$, $p < 0.01$), with more new bone in Group B1 than in Group B2 ($t = 3.126$, $p = 0.009$) and more new bone in Group B2 than in Groups B3 and B4 ($t = 9.948$, $p < 0.001$) (Fig. 7c). Safranin O solid green staining revealed bone and cartilage foci in the new bone in Groups B1 (Fig. 8a) and B2 (Fig. 8b). However, there were no bone and cartilage foci in Group B3 (Fig. 8c) and Group B4 (Fig. 8d).

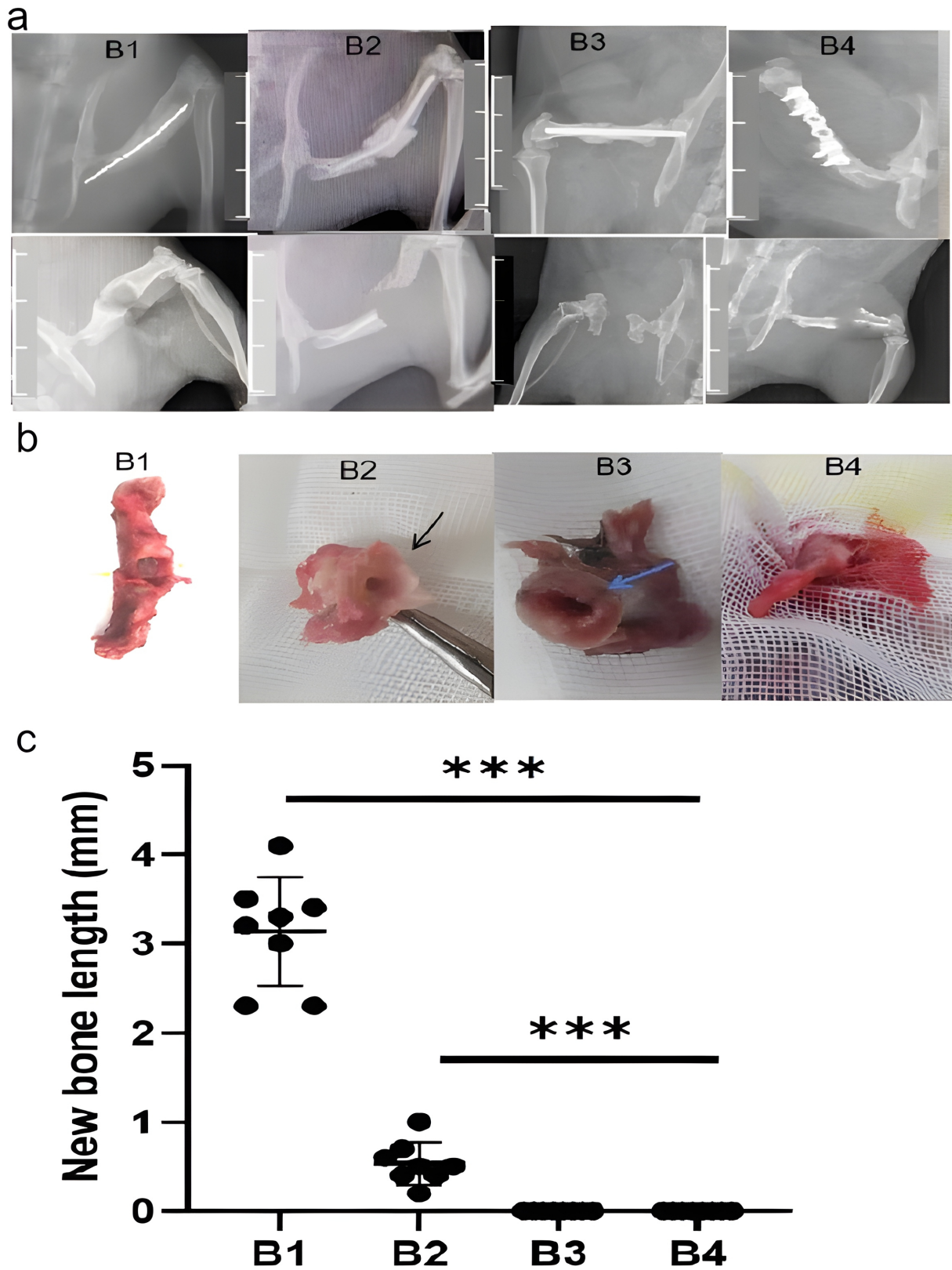


Fig. 7. Osteogenic manifestations at 12 weeks. (a) X-ray and (b) gross examinations showing that more new bone formed from the bone ends and grew along the IM in Group B1 than in Group B2, while Groups B3 and B4 revealed no new bone, and the bone end of Group B4 was wrapped in soft tissue leading to bone atrophy. (c) The new bone among the three groups was significantly different ($n = 12$; mean \pm SD, $***p < 0.001$).

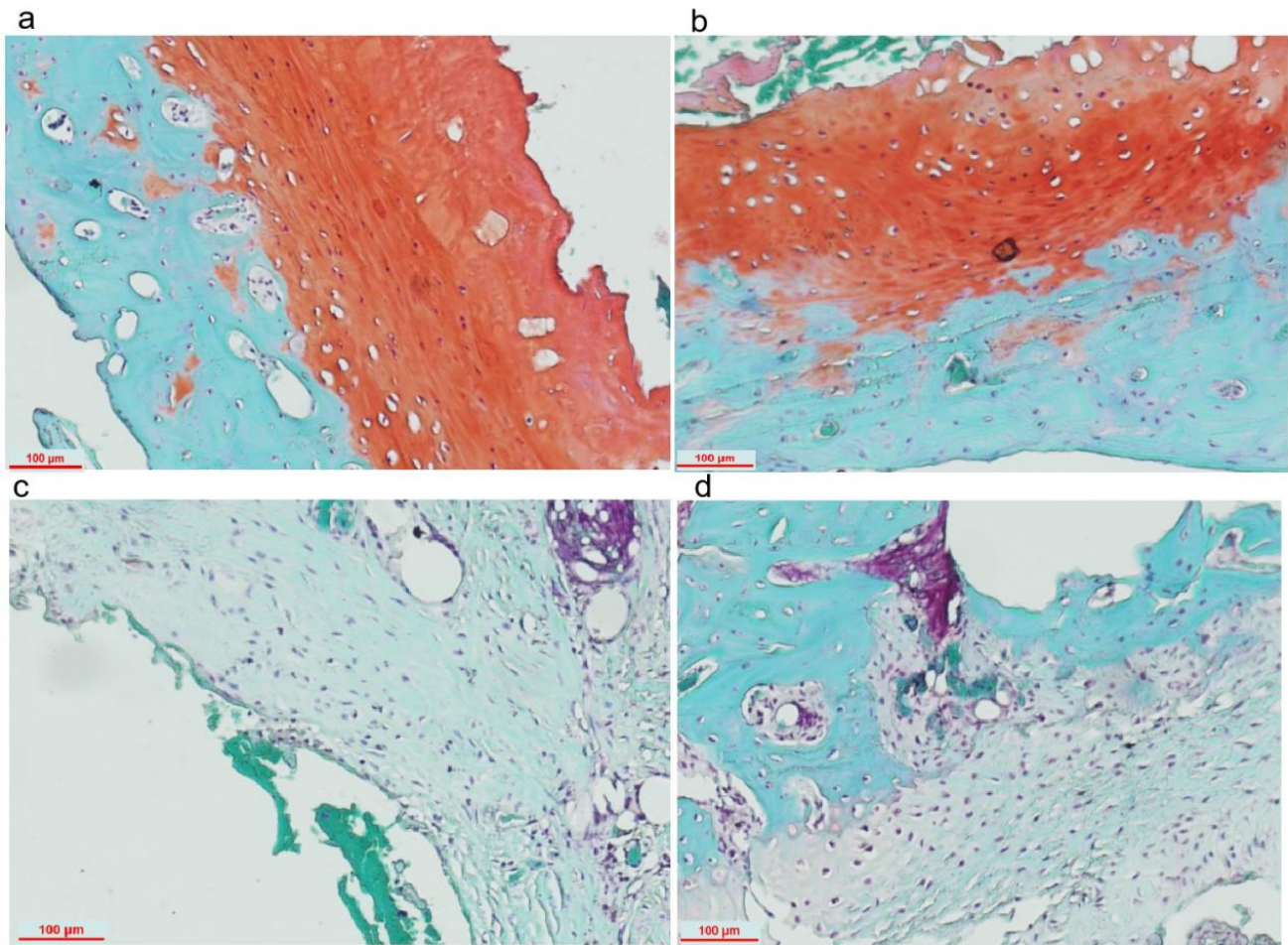


Fig. 8. Safranin O solid green staining of the new bone. Safranin O solid green staining ($\times 100$) showing bone (green) and cartilage (red) foci in the new bone of (a) Group B1 and (b) Group B2, whereas no bone and cartilage foci in (c) Group B3 and (d) Group B4.

Discussion

Giannoudis proposed the “diamond theory”, which refers to the key elements for the successful repair of bone defects and nonunions, including osteoinductive mediators, a bone osteoconduction matrix (scaffold), osteogenic cells, an optimal mechanical environment, a sufficient blood supply, and the resolution of host comorbidities [20]. A lack of any of these elements affects the successful repair of bone defects and nonunions, which has been recognized worldwide. The IMs near the bone end possess all the key elements of the “diamond theory”: ① Osteoinductive mediators: the IM secretes osteogenic factors, including BMP-2, VEGF and TGF- β 1 [8,11,21,22]. ② Osteoconductive matrix: the IM functions as a biological scaffold that mediates the attachment of cells and factors [8,23]. ③ Osteogenic cells: the fresh bone end contains BMSCs derived from the bone marrow and periosteum that can migrate along the IM [24–26]. ④ Rich microvessels: IMs contain microvessels. ⑤ An optimal mechanical environment is provided by internal or external fixation. Therefore, the IMs near the bone end can induce SO.

In this study, the Kirschner wire stimulated the medullary cavity, resulting in overflowing of the bone marrow to the bone ends and the IM. The distal and proximal parts of the IMs in Group A had higher levels of BMSCs and osteogenic and angiogenic factors than did the middle part of the IMs. Group B1 had greater new bone formation, followed by Group B2, while Group B3, with sealed bone marrow, had no new bone formation, i.e., only the IMs near the bone end had more BMSCs and stronger osteogenic activity and SO only developed from the bone end. The osteogenic activities of the IMs correspond to the osteogenic manifestations. This study including two parts indicates that bone marrow overflowing is the key factor for IMGSO. Refer to Fig. 1.

Studies have shown that IMs in ectopic locations (subcutaneously and intramuscularly) also have osteoconductivity, osteoinductivity and microvessels, but do not have osteogenic cells such as BMSCs; therefore, they do not form new bone [23,27]. Although BMSCs can come from the bone marrow and periosteum at the osteotomy site, bone marrow-derived BMSCs are both rapid and abundant. STRO-1 positivity is not the only definitive marker for BM-

SCs, and *in vitro* validation of the role of BMSCs was not performed in this study. However, other studies had verified that the BMSCs of the IMs were mainly derived from the bone marrow of the bone end. An animal experiment conducted by Yin *et al.* [15] revealed that new bone formation within the membrane was significantly delayed and that less bone formation occurred in the group with blocked medullary cavities than in the group without blockage, suggesting that BMSCs, which are derived mainly from the bone marrow, induce SO in the MGBR. Yin *et al.* [16] conducted an experimental study on induced membrane spontaneous osteogenesis (IMSO) of rats by filling different types of cement spacer in bone defects. They found that BMSCs were present in the IMs formed without blocked medullary cavities, whereas BMSCs were absent in the IMs formed with blocked medullary cavities. We agree with the view that rich BMSCs of the IMs mainly come from the bone marrow. The bone marrow contains abundant BMSCs, and percutaneous bone marrow injections have been a bone graft method for treating delayed unions and nonunions, resulting in about 70 % of healing rate [28,29]. The main reason for the unsatisfactory healing rate is that bone marrow cannot accumulate at the fracture site. IM has the characteristics of osteoinduction, osteoconduction and rich blood supply. In addition, IM can wrap and accumulate bone marrow. Therefore, IM combining bone marrow enhances the osteogenic activity of the IM, inducing SO, i.e., producing a $1 + 1 > 2$ effect, and thus requiring little or no material autogenous bone graft. Cuvillier *et al.* [30] reported 12 patients with bone defects after bone resection for chronic osteomyelitis of the femur or tibia, were treated with IMT. The second stage of IMT consisted of the locked intramedullary nail associated with autologous bone marrow graft using the Reamer-Irrigator-Aspirator (RIA) technique. All defects healed at follow-up. Therefore, the combination of IM and bone marrow may be a promising method for treating bone defects.

In addition to the bone marrow, which provides osteogenic cells (mainly BMSCs) and is the key factor of IMGSO, another main influencing factor of IMGSO is the maintenance of an appropriate membrane size. Studies [1,2,6] have shown that the existence and maintenance of the submembrane space are crucial for bone regeneration in MGBR: size mismatching, collapse, displacement, rupture, and premature degradation of the membrane can reduce and remove the space under the membrane, severely hindering bone regeneration and leading to incomplete bone regeneration and even bone nonunion. In this study, a larger spacer in Group B2 interfered with the overflow of the bone marrow to the bone end and did not maintain an appropriate membrane size, which interfered with new bone growth from the bone end, resulting in less new bone.

BMSCs have strong self-renewal and differentiation abilities. During the BMSC differentiation into mature osteoblasts, transcription factors and signaling pathway reg-

ulation are required and play important roles. Research has shown that signaling pathways, including the Wnt/ β -catenin, Notch, BMP/TGF- β , PI3K/Akt/mTOR, mitogen-activated protein kinase (MAPK), PDGF, IGF, FGF, Ca²⁺ and BMP2/Smad pathways, play important roles in the bone regeneration [31,32].

Our histological analysis showed bone and cartilage foci in the new bone, indicating endochondral ossification. In an experiment of rat femoral defects fixed with Kirschner wires and PMMA spacers, Guimarães *et al.* [33] also observed the formation of new bone near the bone end, which was histologically analyzed to contain endochondral ossification, similar to ours.

This study has several limitations. First, this investigation only verified IMGSO and explored its main influencing factors, but the detailed molecular mechanism, which has not been elucidated, advanced techniques such as immunohistochemistry or pathway-specific inhibitors are needed to provide deeper mechanistic insights in future research. Second, STRO-1 positivity is not the only definitive marker for BMSCs, and further verification of its source and function is needed in future studies.

Conclusions

We have demonstrated that the osteogenic activities of different parts of the IMs vary, with the strongest activity in the IM near the bone end. Bone marrow overflowing of the bone end enhances the osteogenic activities of the IMs, resulting in IMGSO, and is the key factor. Another main influencing factor is the maintenance of an appropriate membrane size.

List of Abbreviations

BMSC, bone mesenchymal stem cell; BMP-2, bone morphogenic protein-2; MGBR, membrane-guided bone regeneration; IM, induced membrane; IMGSO, induced membrane-guided spontaneous osteogenesis; IMT, induced membrane technique; IMSO, induced membrane spontaneous osteogenesis; PMMA, polymethyl methacrylate; SD, standard deviation; SO, spontaneous osteogenesis; TGF- β 1, transforming growth factor- β 1; VEGF, vascular endothelial growth factor; MGTR, membrane-guided tissue regeneration; PVDF, polyvinylidene fluoride; qRT-PCR, quantitative RT-PCR.

Availability of Data and Materials

The data that support the findings of this study are available from the corresponding author upon reasonable request.

Author Contributions

QDY and XMC contributed to the design of this work. QDY and JL contributed to the interpretation of data. QDY and XMC analyzed the data. QDY and FYB drafted the

work. JL, QDY and XMC revised critically for important intellectual content. All authors read and approved the final manuscript. All authors agreed to be accountable for all aspects of the work in ensuring that questions related to the accuracy or integrity of any part of the work were appropriately investigated and resolved.

Ethics Approval and Consent to Participate

All applicable international, national, and/or institutional guidelines for the care and use of animals were followed. All procedures performed in studies involving animals were in accordance with the ethical standards of the institution or practice at which the studies were conducted (Registration time: March 15, 2022/No. L2022103).

Acknowledgments

Thanks to Wuxi Huaixin Biomedical Technology Co., Ltd. for the support in stem cell testing for this experiment.

Funding

This study was supported by the top medical expert team of the “Taihu Talent Program” in Wuxi (2020) (WXTTP-202010), the Innovation and Entrepreneurship Program for Excellent Doctorate of Wuxi Ninth People’s Hospital (WX9PH-IEPED-01), the Wuxi Science and Technology Development Fund Project (Y20212014), and the Project of Jiangsu Provincial Health Commission (Z2020010).

Conflict of Interest

The authors declare that they have no competing interests.

References

- [1] Nyman S, Lindhe J, Karring T, Rylander H. New attachment following surgical treatment of human periodontal disease. *Journal of Clinical Periodontology*. 1982; 9: 290–296. <https://doi.org/10.1111/j.1600-051x.1982.tb02095.x>.
- [2] Buser D, Dula K, Belsler U, Hirt HP, Berthold H. Localized ridge augmentation using guided bone regeneration. I. Surgical procedure in the maxilla. *The International Journal of Periodontics & Restorative Dentistry*. 1993; 13: 29–45.
- [3] Calciolari E, Corbella S, Gkraniats N, Viganó M, Sculean A, Donos N. Efficacy of biomaterials for lateral bone augmentation performed with guided bone regeneration. A network meta-analysis. *Periodontology 2000*. 2023; 93: 77–106. <https://doi.org/10.1111/prd.12531>.
- [4] Elgali I, Omar O, Dahlin C, Thomsen P. Guided bone regeneration: materials and biological mechanisms revisited. *European Journal of Oral Sciences*. 2017; 125: 315–337. <https://doi.org/10.1111/eos.12364>.
- [5] Kim BN, Ko YG, Yeo T, Kim EJ, Kwon OK, Kwon OH. Guided Regeneration of Rabbit Calvarial Defects Using Silk Fibroin Nanofiber-Poly(glycolic acid) Hybrid Scaffolds. *ACS Biomaterials Science & Engineering*. 2019; 5: 5266–5272. <https://doi.org/10.1021/acsbomaterials.9b00678>.
- [6] Farso Nielsen F, Karring T, Gogolewski S. Biodegradable guide for bone regeneration. Polyurethane membranes tested in rabbit radius defects. *Acta Orthopaedica Scandinavica*. 1992; 63: 66–69. <https://doi.org/10.3109/17453679209154853>.
- [7] Alford AI, Nicolaou D, Hake M, McBride-Gagyi S. Masquelet’s induced membrane technique: Review of current concepts and future directions. *Journal of Orthopaedic Research: Official Publication of the Orthopaedic Research Society*. 2021; 39: 707–718. <https://doi.org/10.1002/jor.24978>.
- [8] Aurégan JC, Bégue T. Induced membrane for treatment of critical sized bone defect: a review of experimental and clinical experiences. *International Orthopaedics*. 2014; 38: 1971–1978. <https://doi.org/10.1007/s00264-014-2422-y>.
- [9] Grün W, Hansen EJJ, Andreassen GS, Clarke-Jenssen J, Madssen JE. Functional outcomes and health-related quality of life after reconstruction of segmental bone loss in femur and tibia using the induced membrane technique. *Archives of Orthopaedic and Trauma Surgery*. 2023; 143: 4587–4596. <https://doi.org/10.1007/s00402-022-04714-9>.
- [10] Masquelet AC. Induced Membrane Technique: Pearls and Pitfalls. *Journal of Orthopaedic Trauma*. 2017; 31: S36–S38. <https://doi.org/10.1097/BOT.0000000000000979>.
- [11] Wang K, Gao F, Zhang Y, Dai B, Yan X, He X, *et al.* Comparison of osteogenic activity from different parts of induced membrane in the Masquelet technique. *Injury*. 2023; 54: 111022. <https://doi.org/10.1016/j.injury.2023.111022>.
- [12] Klauke K, Knothe U, Anton C, Pfluger DH, Stoddart M, Masquelet AC, *et al.* Bone regeneration in long-bone defects: tissue compartmentalisation? *In vivo study on bone defects in sheep*. *Injury*. 2009; 40: S95–S102. <https://doi.org/10.1016/j.injury.2009.10.043>.
- [13] Gruber HE, Gettys FK, Montijo HE, Starman JS, Bayoumi E, Nelson KJ, *et al.* Genomewide molecular and biologic characterization of biomembrane formation adjacent to a methacrylate spacer in the rat femoral segmental defect model. *Journal of Orthopaedic Trauma*. 2013; 27: 290–297. <https://doi.org/10.1097/BOT.0b013e3182691288>.
- [14] Lu Y, Wang J, Yang Y, Yin Q. Bone defects are repaired by enhanced osteogenic activity of the induced membrane: a case report and literature review. *BMC Musculoskeletal Disorders*. 2021; 22: 447. <https://doi.org/10.1186/s12891-021-04317-2>.
- [15] Yin Q, Chen X, Dai B, Liu J, Yang Y, Song S, *et al.* Varying degrees of spontaneous osteogenesis of Masquelet’s induced membrane: experimental and clinical observations. *BMC Musculoskeletal Disorders*. 2023; 24: 384. <https://doi.org/10.1186/s12891-023-06498-4>.
- [16] Yin Q, Mao D, Rui Y. Experimental study on the causes of spontaneous osteogenesis of Masquelet technique induced membrane. *Zhongguo Xiu Fu Chong Jian Wai Ke Za Zhi = Zhongguo Xiu Fu Chongjian Waike Zazhi = Chinese Journal of Reparative and Reconstructive Surgery*. 2024; 38: 1254–1260. <https://doi.org/10.7507/1002-1892.202403021>.
- [17] Yee MA, Mead MP, Alford AI, Hak DJ, Mauffrey C, Hake ME. Scientific Understanding of the Induced Membrane Technique: Current Status and Future Directions. *Journal of Orthopaedic Trauma*. 2017; 31: S3–S8. <https://doi.org/10.1097/BOT.0000000000000981>.
- [18] Klein C, Monet M, Barbier V, Vanlaeys A, Masquelet AC, Gournon R, *et al.* The Masquelet technique: Current concepts, animal models, and perspectives. *Journal of Tissue Engineering and Regenerative Medicine*. 2020; 14: 1349–1359. <https://doi.org/10.1002/term.3097>.
- [19] Verboket RD, Leiblein M, Janko M, Schaible A, Brune JC, Schröder K, *et al.* From two stages to one: acceleration of the induced membrane (Masquelet) technique using human acellular dermis for the treatment of non-infectious large bone defects. *European Journal of Trauma and Emergency Surgery: Official Publication of the European Trauma Society*. 2020; 46: 317–327. <https://doi.org/10.1007/s00068-019-01296-x>.
- [20] Miska M, Schmidmaier G. Diamond concept for treatment of nonunions and bone defects. *Der Unfallchirurg*. 2020; 123: 679–686. <https://doi.org/10.1007/s00113-020-00843-1>.
- [21] Gindraux F, Loisel F, Bourgeois M, Oudina K, Melin M, de Billy B, *et al.* Induced membrane maintains its osteogenic properties even

- when the second stage of Masquelet's technique is performed later. *European Journal of Trauma and Emergency Surgery: Official Publication of the European Trauma Society*. 2020; 46: 301–312. <https://doi.org/10.1007/s00068-019-01184-4>.
- [22] Stahl A, Park YB, Park SH, Lin S, Pan CC, Kim S, *et al.* Probing the role of methyl methacrylate release from spacer materials in induced membrane bone healing. *Journal of Orthopaedic Research: Official Publication of the Orthopaedic Research Society*. 2022; 40: 1065–1074. <https://doi.org/10.1002/jor.25147>.
- [23] Pélissier P, Lefevre Y, Delmond S, Villars F, Vilamitjana-Amedee J. Influences of induced membranes on heterotopic bone formation within an osteo-inductive complex. *Experimental study in rabbits. Annales de Chirurgie Plastique et Esthétique*. 2009; 54: 16–20. <https://doi.org/10.1016/j.anplas.2008.07.001>.
- [24] Henrich D, Seebach C, Nau C, Basan S, Relja B, Wilhelm K, *et al.* Establishment and characterization of the Masquelet induced membrane technique in a rat femur critical-sized defect model. *Journal of Tissue Engineering and Regenerative Medicine*. 2016; 10: E382–E396. <https://doi.org/10.1002/term.1826>.
- [25] Mathieu L, Murison JC, de Rousiers A, de l'Escalopier N, Lutomski D, Collombet JM, *et al.* The Masquelet Technique: Can Disposable Polypropylene Syringes be an Alternative to Standard PMMA Spacers? A Rat Bone Defect Model. *Clinical Orthopaedics and Related Research*. 2021; 479: 2737–2751. <https://doi.org/10.1097/COOR.0000000000001939>.
- [26] Tang Q, Tong M, Zheng G, Shen L, Shang P, Liu H. Masquelet's induced membrane promotes the osteogenic differentiation of bone marrow mesenchymal stem cells by activating the Smad and MAPK pathways. *American Journal of Translational Research*. 2018; 10: 1211–1219.
- [27] Catros S, Zwetyenga N, Bareille R, Brouillaud B, Renard M, Amédée J, *et al.* Subcutaneous-induced membranes have no osteoinductive effect on macroporous HA-TCP *in vivo*. *Journal of Orthopaedic Research: Official Publication of the Orthopaedic Research Society*. 2009; 27: 155–161. <https://doi.org/10.1002/jor.20738>.
- [28] Lana JF, da Fonseca LF, Azzini G, Santos G, Braga M, Cardoso Junior AM, *et al.* Bone Marrow Aspirate Matrix: A Convenient Ally in Regenerative Medicine. *International Journal of Molecular Sciences*. 2021; 22: 2762. <https://doi.org/10.3390/ijms22052762>.
- [29] Salamanna F, Contartese D, Nicoli Aldini N, Barbanti Brodano G, Griffoni C, Gasbarrini A, *et al.* Bone marrow aspirate clot: A technical complication or a smart approach for musculoskeletal tissue regeneration? *Journal of Cellular Physiology*. 2018; 233: 2723–2732. <https://doi.org/10.1002/jcp.26065>.
- [30] Cuvillier M, Meucci JF, Cazorla C, Carricajo A, Neri T, Boyer B. Masquelet's induced membrane technique associated with Reamer Irrigation Aspiration grafting and intramedullary Nailing (MaRIAN) for chronic diaphyseal osteomyelitis of the lower limb. *Orthopaedics & Traumatology, Surgery & Research: OTSR*. 2022; 108: 103395. <https://doi.org/10.1016/j.otsr.2022.103395>.
- [31] Kim BS, Kang HJ, Park JY, Lee J. Fucoidan promotes osteoblast differentiation via JNK- and ERK-dependent BMP2-Smad 1/5/8 signaling in human mesenchymal stem cells. *Experimental & Molecular Medicine*. 2015; 47: e128. <https://doi.org/10.1038/emm.2014.95>.
- [32] Majidinia M, Sadeghpour A, Yousefi B. The roles of signaling pathways in bone repair and regeneration. *Journal of Cellular Physiology*. 2018; 233: 2937–2948. <https://doi.org/10.1002/jcp.26042>.
- [33] Guimarães JAM, Scorza BJB, Machado JAP, Cavalcanti ADS, Duarte MEL. Characterization of the Masquelet Induced Membrane Technique in a Murine Segmental Bone Defect Model. *Revista Brasileira de Ortopedia*. 2023; 58: e798–e807. <https://doi.org/10.1055/s-0043-1771490>.

Editor's note: The Scientific Editor responsible for this paper was Chris Evans.

Received: 8th October 2024; **Accepted:** 10th December 2024; **Published:** 14th February 2025